2021 43rd Annual International Conference of the
IEEE Engineering in Medicine & Biology Society (EMBC)
Oct 31 - Nov 4, 2021. Virtual Conference

Customized Total Variation Algorithm for Metal Artifact Reduction in Computed Tomography

Ziheng Deng, Yufu Zhou, Weikang Zhang, Zefan Lin and Jun Zhao*, *Member, IEEE*

Abstract— **Metal artifact reduction (MAR) is a challenge for commercial CT systems. The metal objects of high density adversely affect the measurement process and bring difficulties to image reconstruction. Compressed sensing (CS) reconstruction algorithms have been successfully applied in MAR. Ideally, the desired anatomical information can be restored from incomplete projection data. However, in most practical cases, these conventional CS algorithms may instead introduce severe secondary artifacts due to improper prior information. In this paper, we propose a customized total variation (CTV) method to reduce the metal artifacts based on the specific pattern of the artifacts. The gradient operator within the TV norm is redefined according to the distribution of both the metal objects and tissues for each MAR case. We also provide a weighting strategy to further protect the fine details. Experimental results show that the CTV method achieves better performances than those of the conventional methods.**

I. Introduction

Metal implants in patients would cause severe imaging artifacts during CT scans due to the strong attenuation of metal material. Besides the X-rays passing through the metal implants, the remaining projection data might also be contaminated by beam hardening effect and photon scattering. Many studies have been devoted to metal artifact reduction (MAR). One simple and commonly adopted approach for MAR is to remove the unreliable projections during the image reconstruction [1]. However, additional effort should be made to solve the problem of incomplete data to avoid new artifacts.

Compressed sensing (CS) based reconstruction algorithms achieve much better performance even with highly incomplete projection data [2]. CS theory recovers image signals by introducing a specific transformation from the image domain to a signal-sparse domain. Among them, the total variation (TV) minimization algorithm enjoys great fame and has been applied successively to many fields [3]. The work assumes that most anatomical structures in clinical images are piecewise constant and thereby most noise artifacts are reduced. However, it achieves limited success in the MAR problem. Unlike many other CT image artifacts, metal artifacts are highly inhomogeneous. Since the contaminated projection data is excluded during the image reconstruction process, the measurements of tissues along these projection lines are absent. As a result, the fine details tangent to these projections will not be fully recovered [4]. Moreover, secondary artifacts are introduced by iterative reconstruction algorithms. When an improper initial guess is adopted for the iterative algorithm, the errors in CT values will then leak to adjacent pixels during the projection and back-projection process [5]. Due to data incompleteness, these errors may not be corrected and a series of intensity leakages will then accumulate to severe streak artifacts tangent to the removed projection lines. An example of the streak artifacts is given in Fig. 1(c). Such artifacts are insensitive to gradient operators along the streak's direction, thereby conventional TV regularization turns out to be an inefficient way to reduce metal artifacts.

Several modified TV regularizations have been proposed to fit different needs. Chen *et al.* developed an anisotropic TV norm for limited-angle CT [6]. Based on their observation, the direction of streak artifacts can be predicted according to the scan trajectory. Under this assumption, they designed an extra 1D TV norm adapted to the scan trajectory. Besides, numerous weighting strategies have been introduced to improve the conventional TV algorithm [7] [8]. These methods make efforts in striking the balance between artifact reduction and detail preservation.

To improve the algorithms further, we adjust the TV norm for the MAR problem. In the context of metal artifacts, the directions of the removed projection lines vary from pixel to pixel, which contributes to tricky star-shaped artifacts around the metal objects. However, since all the removed projection lines pass through the metal objects, the distribution of the streak artifacts is still predictable for each specific case. In this paper, we propose a customized TV (CTV) norm constrained iterative algorithm. To reduce the characteristic metal artifacts, we first construct a direction map to estimate the distribution of the potential artifacts. Then the CTV norm with pixel-specific direction is determined according to the map. By exploiting the knowledge of metal objects and background images, we further apply a weighting strategy to preserve the fine details. In Section II, we introduce the implementation details of the CTV method. Experiments on different CT images are conducted in Section III. Finally, we draw the conclusion in Section IV.

II. Methods

A. Optimization model of the CTV algorithm

The conventional TV constrained CT image reconstruction problem can be described as:

$$\min_f \|f\|_{TV} \ \ subject\ to\ \ Af = p \tag{1}$$

where A denotes the system matrix, f is the image vector to be reconstructed, $\|f\|_{TV}$ is the conventional TV norm of image f and p is the adopted measured projection data. Other projections that are contaminated by the metal objects are discarded. The contaminated projection data can be recognized

Research supported by the National Key Research and Development Program (2016YFC0104604, 2016YFC0104608). *Asterisk indicates corresponding author.*

Ziheng Deng, Yufu Zhou, Weikang Zhang, Zefan Lin and *Jun Zhao are with the School of Biomedical Engineering, Shanghai Jiao Tong University, China (*corresponding author Jun Zhao: junzhao@sjtu.edu.cn).

by reprojecting the metal objects that are segmented from the uncorrected image. We rewrite (1) with CTV regularization into an unconstrained optimization form:

$$\min_f \frac{\mu}{2}\|Af - p\|_2^2 + (1-\lambda)\|f\|_{TV} + \lambda\|f\|_{cTV} \quad (2)$$

where μ is the Lagrange multiplier, and λ is the variable weight that balances the two regularization terms. The CTV norm $\|f\|_{cTV}$ is defined as:

$$\|f\|_{cTV} = \sum_{x,y}\sum_n W_{n,x,y}\left\|\nabla_{\alpha_{n,x,y}} f(x,y)\right\|_1 \quad (3)$$

x and y are pixel indices and n is the number of metal objects. $W_{n,x,y}$ is the pixel-specific weight, and $\nabla_{\alpha_{n,x,y}}$ is the local gradient operator along a specific direction α.

B. Pixel-specific 1D TV norm

Although the bright and dark streak artifacts with low frequency are visible to human beings, they may confuse the conventional TV algorithm. For example, regions within the streak artifacts are likely to meet the assumption of piecewise constant along the streak's direction. Therefore, TV regularization along such direction contributes little to artifact reduction. On the other hand, the normal direction becomes the Achilles heel of streak artifacts. The 1D TV norm can be used to enforce homogeneity along any designated direction. By this means, it is rational to detect and remove the artifacts using 1D TV norm along the streak's normal direction. Given that the metal artifacts appear to be metal-centered, the shapes of the artifacts are highly relevant to the geometry information of the metal objects. Thus, in the CTV algorithm, we first identify the metal objects using a threshold-based method. Then, for each separate metal object, a direction map is acquired to design a pixel-specific 1D TV norm. For pixel $f(x,y)$, the removed projection line passes through both the pixel and the centroid of the metal can be denoted as:

$$Xcos\theta + Ysin\theta = t\,, 0 \le \theta < \pi \quad (4)$$

where θ is the angle of the projection line. According to the above conclusions, θ reveals the direction of the potential streak artifacts around pixel $f(x,y)$. To enforce homogeneity along streak's normal direction, the direction α in formula (3) is obtained by:

$$\alpha = \begin{cases} \theta + \frac{\pi}{2}, & 0 \le \theta < \frac{\pi}{2} \\ \theta - \frac{\pi}{2}, & \frac{\pi}{2} \le \theta < \pi \end{cases} \quad (5)$$

By traversing the whole image, we collect all the α-directions to construct the direction map and then determine the directions of the CTV norm. Fig. 1 gives an illustration of the CTV norm. The segmented metal objects are marked in red. Note that the direction map in Fig. 1(e) correctly describes the streaks' normal directions shown in Fig. 1(d). Linear interpolation strategy is adopted to apply gradient operator along radial direction since CT images are defined in the Cartesian coordinate system.

C. Weighting strategy

Though the TV minimization algorithm receives widespread acceptance for its capability to reduce artifacts, it is also criticized for the undesired staircase effect which severely blurs the images when inappropriate parameters are adopted. To deal with this problem, we proposed an adaptive weighting strategy for the CTV norm utilizing the information of both the metal objects and the background image.

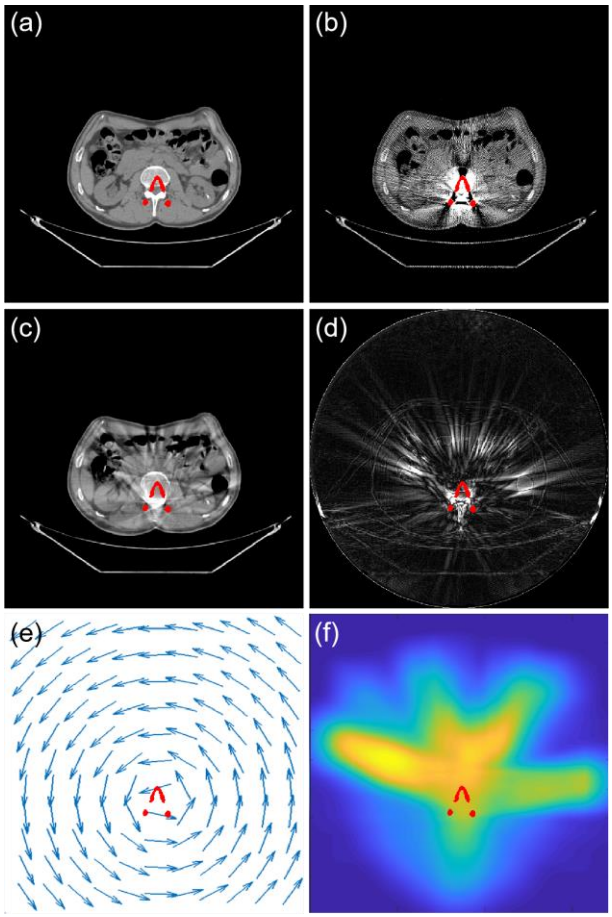

Figure 1. Illustration of the CTV norm. (a) the ground truth, (b) the uncorrected image, (c) the linear interpolation MAR [7] pre-corrected image, (d) the residual image of the pre-corrected image from ground truth, (e) the direction map of the CTV norm, (f) the weighting map of the CTV norm. Red pixels stand for the inserted metal implants.

Based on the analysis above, the streak artifacts originate from the blurring of high-frequency details. Therefore, it is practical to predict the distribution of the streak artifacts before reconstruction. For example, severe artifacts are more likely to be observed within regions that contain rich structure information. These regions thereby require larger CTV parameters to reduce artifact. In this way, we reweight the CTV norm according to the intensity fluctuation along the removed projection line.

To investigate the tissue information in the background image, we first applied conventional linear interpolation MAR (LI-MAR) [9] algorithm to obtain a pre-corrected image $\hat{f}$. After that, a profile $pr_{x,y}$ (s) is drawn for each pixel $\hat{f}(x,y)$ along the projection line defined in formula (4), denoted as:

$$pr_{x,y,n}(s) = \hat{f}(x + scos\theta, y + ssin\theta) \quad (6)$$

To assess the fluctuation of the profile, we further calculate the absolute value of the normalized profile:

$$\widehat{pr}_{x,y,n}(s) = \left|pr_{x,y,n}(s) - \overline{pr}_{x,y,n}\right| \quad (7)$$

where $\overline{pr}_{x,y}$ is the mean value of the profile. The pixel-specific weight in formula (3) is then given by:

$$W_{n,x,y} = \sum_s \widehat{pr}_{x,y,n}(s)K(s) \qquad (8)$$

where $K(s)$ is a 1-D Gaussian kernel to introduce a distance weight. The weighting map in Fig. 1(f) shows its ability to predict the distribution of streak artifacts before reconstruction.

III. Results

The proposed CTV algorithm is evaluated on simulated images. We followed Zhang's procedure [10] to simulate metal-induced projection data and used real clinical images from "the 2016 Low-dose CT Grand Challenge" dataset [11]. The size of the reconstructed CT image is 512×512. A fan-beam geometry CT scan is simulated and 512 projection views are sampled evenly from 0° to 360° with a flat detector of 768 bins. The metal implants are assumed to be titanium to simulate the beam-hardening effect. As for the Poisson noise, we assumed that the X-ray has 2×10^7 photons. The Institution's Ethical Review Board approved all experimental procedures involving human subjects.

In our experiment, problem (2) is solved in the Split-Bregman framework [12], and the conjugate gradient (CG) method is used for the subproblem. The maximum iteration number of the main loop is 25, and we performed 20 CG iterations within each loop. Considering that the weighting strategy for the CTV algorithm may lead to nonuniform resolution, the parameter λ in (2) is initialized as 1 and then gradually decreased as the iteration progresses. Several other methods were compared with the proposed algorithm. The normalized MAR (NMAR) [13] is a state-of-the-art analytic algorithm. The LI-MAR pre-corrected results are provided for the NMAR algorithm as prior images to improve performance. Besides the conventional TV algorithm, the weighted TV (WTV) algorithm [14] designed for the MAR problem is also included.

Fig. 2 shows the reconstruction results for an abdominal CT image with metal implants. NMAR partly reduces the metal artifacts, but it inevitably introduces severe secondary artifacts. All three iterative algorithms achieve better results at the cost of computation time. The WTV algorithm avoids most

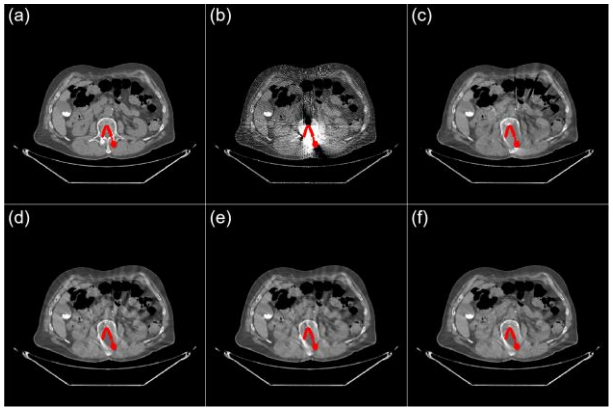

Figure 2. Reconstructed abdominal CT images. Comparisons of (a) the ground truth, (b) the uncorrected image, (c) NMAR result, (d) conventional TV result, (e) WTV result, (f) CTV result. The display window is [-200,300] HU.

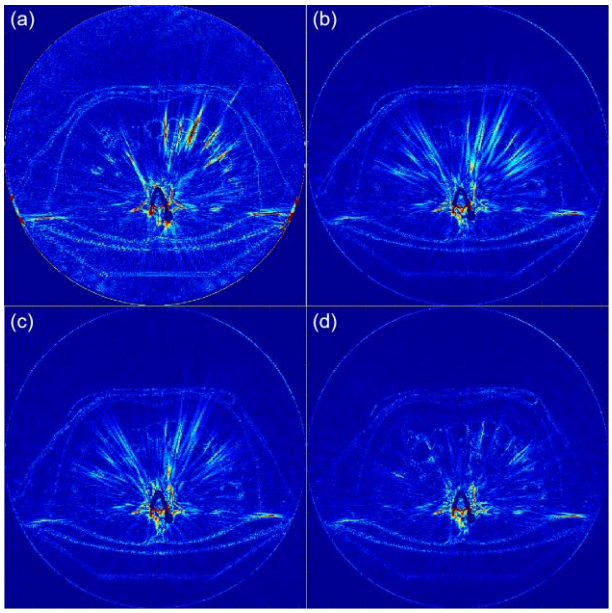

Figure 3. Residual images from the ground truth. (a) NMAR result, (b) conventional TV result, (c) WTV result, (d) CTV result. The display window is [0,200] HU.

of the artifacts in regions around the metal implants, however, it fails to reduce the streak artifacts that distributed widely. The proposed CTV algorithm outperforms the others due to its specially designed regularization term. RMSE values of NMAR, TV, WTV, CTV images are 36.57, 28.56, 27.81, 25.16 HU respectively, which is consistent with the visual inspection.

Fig. 3 shows the residual images from the ground truth. Star-shaped artifacts are easily observed in all the compared algorithms, which degrade the quality of images with great errors and might lead to wrong structures in the results. On the contrary, our CTV algorithm is capable of dealing with these streak artifacts.

We further investigate the effectiveness of the proposed CTV method in the context of multiple metal objects. As shown in Fig. 4, different numbers of dental fillings are inserted into the same CT image. Artifacts caused by a single metal object can be easily removed using any of these iterative algorithms or the NMAR algorithm. As the number of dental fillings increases, severe streak artifacts appear and distort the anatomic information. All the three compared algorithms introduce fake structures in case 2 and case 3. The proposed CTV algorithm provides a satisfactory result for case 2 and removes most of the artifacts in case 3.

Table I gives the quantitative assessment in region of interest (ROI) for three iterative algorithms. Conventional TV algorithm mistakes several streak artifacts as real structures, which results in the highest reconstruction errors. The WTV algorithm assumes that pixels near the metal region are less accurate and assigns higher TV weight to regions around the metal implants. However, it obtains low structural similarity because it blurs the ROI severely but still retains the streak artifacts. Our CTV algorithm gets the best quantitative performances in all three cases.

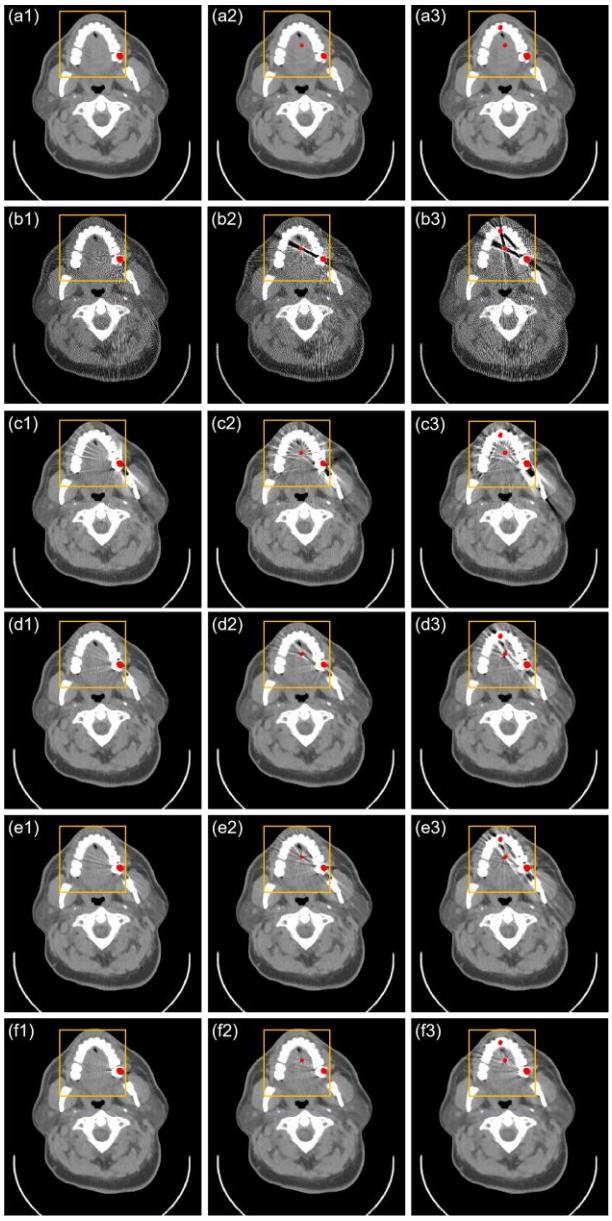

Figure 4. Reconstructed dental CT images. Each column is corresponding to one case with different number of dental fillings. Rows from top to bottom are (a) ground truth images, (b) uncorrected images, (c) NMAR results, (d) conventional TV results, (e) WTV results and (f) CTV results. The display window is [-200,300] HU. The region of interest is marked with a yellow box.

TABLE I. QUANTITATIVE ASSESSMENT IN REGION OF INTEREST FOR DIFFERENT ALGORITHMS

		TV	WTV	CTV
Case 1	RMSE	73.91	69.92	**66.99**
	SSIM	0.9576	0.9614	**0.9705**
Case 2	RMSE	79.73	74.13	**67.17**
	SSIM	0.9424	0.9436	**0.9659**
Case 3	RMSE	138.66	129.47	**108.26**
	SSIM	0.8842	0.8893	**0.9341**

*Unit of RMSE: HU

IV. DISCUSSIONS AND CONCLUSION

The appearance of metal artifacts varies case by case. However, homogenous regularization terms are adopted by most iterative algorithms. In this work, we have proposed a CTV norm constrained iterative algorithm for metal artifact reduction. Based on the understanding of the image reconstruction process, we utilize the spatial information of both the metal objects and tissues to predict the distribution of streak artifacts. Then, a pixel-specific CTV norm is designed to reduce the artifacts and preserve the fine structures. Experimental results show the higher performance of our method.

For further thought, since the CTV method only modifies the regularization term, it can be easily combined with other advanced MAR algorithms to even improve the efficacy while reducing the computation time. Besides, the proposed CTV method can also be extended and applied to other CT image reconstruction cases where prior knowledge of artifact distribution exists.

REFERENCES

[1] L. Gjesteby et al., "Metal artifact reduction in CT: where are we after four decades?," Ieee Access, vol. 4, pp. 5826-5849, 2016.
[2] S. Ravishankar, J. C. Ye, and J. A. Fessler, "Image reconstruction: From sparsity to data-adaptive methods and machine learning," Proceedings of the IEEE, vol. 108, no. 1, pp. 86-109, 2019.
[3] E. Y. Sidky and X. Pan, "Image reconstruction in circular cone-beam computed tomography by constrained, total-variation minimization," Physics in Medicine & Biology, vol. 53, no. 17, p. 4777, 2008.
[4] J. Frikel and E. T. Quinto, "Characterization and reduction of artifacts in limited angle tomography," Inverse Problems, vol. 29, no. 12, p. 125007, 2013.
[5] Y. Huang, O. Taubmann, X. Huang, V. Haase, G. Lauritsch, and A. Maier, "Scale-space anisotropic total variation for limited angle tomography," IEEE Transactions on Radiation and Plasma Medical Sciences, vol. 2, no. 4, pp. 307-314, 2018.
[6] Z. Chen, X. Jin, L. Li, and G. Wang, "A limited-angle CT reconstruction method based on anisotropic TV minimization," Physics in Medicine & Biology, vol. 58, no. 7, p. 2119, 2013.
[7] E. J. Candes, M. B. Wakin, and S. P. Boyd, "Enhancing sparsity by reweighted ℓ 1 minimization," Journal of Fourier analysis and applications, vol. 14, no. 5-6, pp. 877-905, 2008.
[8] Y. Liu, J. Ma, Y. Fan, and Z. Liang, "Adaptive-weighted total variation minimization for sparse data toward low-dose x-ray computed tomography image reconstruction," Physics in Medicine & Biology, vol. 57, no. 23, p. 7923, 2012.
[9] D. Prell, W. Kalender, and Y. Kyriakou, "Development, implementation and evaluation of a dedicated metal artefact reduction method for interventional flat-detector CT," The British journal of radiology, vol. 83, no. 996, pp. 1052-1062, 2010.
[10] Y. Zhang and H. Yu, "Convolutional neural network based metal artifact reduction in x-ray computed tomography," IEEE transactions on medical imaging, vol. 37, no. 6, pp. 1370-1381, 2018.
[11] C. McCollough et al., "Low Dose CT Image and Projection Data [Data set]," The Cancer Imaging Archive, 2020.
[12] S. Ramani and J. A. Fessler, "A splitting-based iterative algorithm for accelerated statistical X-ray CT reconstruction," IEEE transactions on medical imaging, vol. 31, no. 3, pp. 677-688, 2011.
[13] E. Meyer, R. Raupach, M. Lell, B. Schmidt, and M. Kachelrieß, "Normalized metal artifact reduction (NMAR) in computed tomography," Medical physics, vol. 37, no. 10, pp. 5482-5493, 2010.
[14] Y. Zhang, X. Mou, and H. Yan, "Weighted total variation constrained reconstruction for reduction of metal artifact in CT," in IEEE Nuclear Science Symposuim & Medical Imaging Conference, 2010: IEEE, pp. 2630-2634.